Coordinating Tectons: Bipyridyl Terminated Allenylidene Complexes

Marie P. Cifuentes,[†] Mark G. Humphrey,[†] George A. Koutsantonis,*[,‡] Nigel A. Lengkeek,[‡] Simon Petrie,[†] Vanessa Sanford,[‡] Phil A. Schauer,[‡] Brian W. Skelton,[‡] Robert Stranger,[†] and Allan H. White[‡]

Chemistry, M313, School of Biomedical, Biomolecular and Chemical Sciences, The University of Western Australia, Crawley, WA, 6009, Australia, and Department of Chemistry, Australian National University, Canberra, ACT, 0200, Australia

Received August 13, 2007

A series of complexes with π-conjugated carbon chains terminated by bipyridyl moieties has been prepared. These allenylidene complexes were derived from 9-hydroxy-9-ethynyl-4,5-diazafluorene, the preparation of which is reported; the new allenylidene complexes are highly colored with the cumulated carbon chain terminating in a bipyridyl unit providing a site for further coordination. The synthesis, characterization, and X-ray structure determination of *trans*-[MCl(P∩P)$_2$═C═C═(4,5-diazafluoren-9-yl)]PF$_6$ (M = Ru, P∩P = bis(diphenylphosphino)methane (dppm), 1,2-bis(diphenylphosphino)ethane (dppe), 1,2-bis(dimethylphosphino)ethane (dmpe); M = Os, P∩P = dppm) are described. The effect of the variation in metal and ligand on electronic and electrochemical characteristics of these complexes has been investigated by using UV–vis, solution electrochemistry, and a combination of these techniques in spectroelectrochemical experiments. DFT calculations have been performed on *trans*-[RuCl(P∩P)$_2$═C═C═(4,5-diazafluoren-9-yl)]^q (P∩P = dppm, bis(dimethylphosphino)methane (dmpm); $q = -1$, 0, +1, +2) and subsequently solvent-corrected calculations with use of COSMO were also undertaken to examine the nature of electronic transitions in various oxidation states.

Introduction

The diversity of purpose required by the next generation of functional materials has ensured a critical role for transition metals in materials science,[1] as their varied properties ensure diverse levels of functionality can be incorporated which can be invoked photochemically and electrochemically.[2] The range of materials into which transition metal centers are now being incorporated is vast and includes liquid crystalline materials,[1,3] metallomicelles,[4] nonlinear optical materials,[5–7] molecular wires/switches,[2] chromophore-quencher compounds,[8] dye-sensitized photovoltaic cells,[9] and organic light-emitting diodes.[10]

The roles played by metals in materials are still evolving and there is an increasing effort to incorporate redox-active centers into many materials, e.g., conducting polymers, in attempts to create highly efficient redox conductivities for sensors, catalytic, photochemical, and photoelectronic applications.[11] However, in conducting metallopolymers "*an understanding of the interactive roles that the metal centres and the organic polymer backbone play is in its early stages*",[11] and thus much fundamental work remains to be done to provide a firm background to future applications.

One of the important variables is the nature of the redox center: there are obviously substantial numbers of metal complexes whose photophysical and electrochemical properties are well-known that can be recruited to the purpose, e.g., ruthenium polypyridyl compounds (photochemical)[12] or lanthanide macrocycles (luminescent),[13] and the ubiquitous metallocenes, particularly, ferrocene.[14,15] In this latter case, ferrocene has been used because it has a well-understood and developed chemistry and is capable of undergoing a reversible one-electron oxidation, albeit giving the ferrocenium ion, which lacks the stability of ferrocene. However, as a tool for the construction of materials, it is unparalleled because of its predictability.[16]

Our approach encompasses organometallic coordination chemistry, in the knowledge that metal ion coordination is one

* Corresponding author. E-mail: gak@chem.uwa.edu.au.
[†] Australian National University.
[‡] The University of Western Australia.

(1) Donnio, B. *Curr. Opin. Colloid Interface Sci.* **2002**, *7*, 371.
(2) Low, P. J. *Dalton Trans.* **2005**, 2821.
(3) Piguet, C.; Bunzli, J.-C.; Donnio, B.; Guillion, D. *Chem. Commun.* **2006**, 3755.
(4) Griffiths, P. C.; Fallis, I. A.; Willock, D. J.; Paul, A.; Barrie, C. L.; Griffiths, P. M.; Williams, G. M.; King, S. M.; Heenan, R. K.; Goergl, R. *Chem. Eur. J.* **2004**, *10*, 2022.
(5) Cifuentes, M. P.; Powell, C. E.; Morrall, J. P.; McDonagh, A. M.; Lucas, N. T.; Humphrey, M. G.; Samoc, M.; Houbrechts, S.; Asselberghs, I.; Clays, K.; Persoons, A.; Isoshima, T. *J. Am. Chem. Soc.* **2006**, *128*, 10819.
(6) Cifuentes, M. P.; Humphrey, M. G. *J. Organomet. Chem.* **2004**, *689*, 3968.
(7) Powell, C. E.; Humphrey, M. G. *Coord. Chem. Rev.* **2004**, *248*, 725.
(8) Flamigni, L.; Barigelletti, F.; Armaroli, N.; Collin, J.-P.; Dixon, I. M.; Sauvage, J.-P.; Williams, J. A. G. *Coord. Chem. Rev.* **1999**, *671*, 190–192.
(9) Nazeerudin, M. K.; Graetzel, M. In *Comprehensive Coordination Chemistry II*; McCleverty, J. A., Meyer, T. J., Eds.; Elsevier-Pergamon: Oxford, UK, 2004; Vol. 9, p 719.
(10) Coe, B. J.; Curati, N. R. M. *Comments Inorg. Chem.* **2004**, *25*, 147.
(11) Holliday, B. J.; Swager, T. M. *Chem. Commun.* **2005**, 23.
(12) Bonnet, S.; Collin, J.-P.; Sauvage, J.-P. *Chem. Commun.* **2005**, *25*, 3195.
(13) Callan, J. F.; de Silva, A. P.; Magri, D. C. *Tetrahedron* **2005**, *61*, 8551.
(14) Ganesan, N.; Gadre, A. P.; Paranjape, M.; Currie, J. F. *Anal. Biochem.* **2005**, *343*, 188.
(15) Evans, A. J.; Matthews, S. E.; Cowley, A. R.; Beer, P. D. *Dalton Trans.* **2003**, 4644.
(16) Togni, A.; Hayashi, T., *Ferrocenes: homogeneous catalysis, organic synthesis, materials science*; VCH: New York, 1995; p 540.

10.1021/om700824g CCC: $40.75
Publication on Web 03/19/2008

of the most powerful mechanisms for the spatial ordering of organic ligands. We seek to construct organometallic complexes that contain conjugated carbon ligands with additional coordination sites (tectons) that will allow the construction of polymers.

We chose to study the allenylidene ligand which is conjugated through to the metal center and have targeted bis-allenylidene complexes. Metallacumulenes have elicited interest in the chemical community for over forty years, first demonstrating their symbiosis with carbon analogues, and, as synthetic ingenuity developed, with increasingly longer cumulated chains being prepared. These molecules often owe their existence to coordination to the metal centers which stabilize them sufficiently for characterization. The allenylidene complexes have been studied less than the C_1 and C_2 homologues, although the literature has been extensively reviewed over recent years with annual surveys,[17–22] allenylidenes and higher cumulenylidenes reviewed in detail,[23,24] polymetallic C_n systems,[25] C_{3-5} ruthenium cumulenylidenes,[26] iridium cumulenylidenes,[27] and rhodium allenylidenes[28] being the most relevant. The seminal contributions of Selegue[29] and Berke[30] provided the first examples and, in the case of the former, a general route to these compounds.

Herein, we describe our investigations into the synthesis of conjugated allenylidene complexes terminated by coordinating bipyridyl tectons and their physical properties.

Experimental Section

General Considerations. Samples for infrared spectroscopy were prepared as pellets (KBr) or Nujol mulls (NaCl plates), with spectra acquired on Bio-Rad FTS-45 or DigiLab Excalibur FTS-3000 spectrometers. UV–vis spectra were obtained by using a Hewlett-Packard 8452A diode-array spectrophotometer from solutions in quartz cuvettes. ^{1}H, ^{13}C{^{1}H}, and ^{31}P{^{1}H} nuclear magnetic resonance spectra were acquired on Bruker ARX-300, AV-500, or AV-600 spectrometers and referenced with respect to residual solvent signals or an external capillary of 85% H_3PO_4 for ^{31}P NMR spectra. Mass spectra were acquired on a VG Autospec spectrometer employing the Fast-Atom-Bombardment (FAB) or Electron-Impact (EI) techniques. Elemental analyses were performed by Microanalytical Services, Research School of Chemistry, Australian National University, Canberra, Australia. 4,5-Diazafluoren-9-one was prepared from 1,10-phenanthroline (Aldrich) by the literature procedure.[31] The complexes *cis*-[$RuCl_2$(dppm)$_2$], *cis*-[$RuCl_2$(dppe)$_2$], [$RuCl_2$(dmpe)$_2$], and [$OsCl_2$(dppm)$_2$] were prepared from [$RuCl_2$(dmso)$_4$] and [$OsCl_2(PPh_3)_3$], respectively, in hot toluene.[32] ^{n}BuLi (2.0 M in cyclohexane, Sigma-Aldrich), ClMgC≡CH (0.5 M in thf, Sigma-Aldrich), $NaPF_6$ (Sigma-Aldrich), and KPF_6 (BDH) were used as received. Acetylene gas (CIG industries) was freed of acetone by successive passage through dry ice/acetone, concentrated sulfuric acid, and soda lime traps, then bubbled directly into the reaction vessel. Column chromatography was performed with use of silica gel (230–400 mesh ASTM, Merck) as the stationary phase. Solvents for chromatography and general workup procedures were distilled prior to use, while solvents for Schlenk reactions were dried and purified by appropriate means[33] prior to distillation and storage under an atmosphere of high-purity argon. Unless otherwise stated, all reactions were performed under an atmosphere of high-purity argon utilizing standard Schlenk techniques.

Compound 1, 9-Hydroxy-9-ethynyl-4,5-diazafluorene. Method A: LiC≡CH was prepared in situ by the method of Midland[34] and used immediately. In a 500 mL round-bottomed flask thf (130 mL) was saturated with C_2H_2 gas over approximately an hour at −78 °C (CO_2/Me_2CO). To this solution was added ^{n}BuLi (1.10 M in cyclohexane, 8.2 mL, 9.0 mmol) and the resulting solution was left to stir for 30 min. A solution of 4,5-diazafluoren-9-one (1.48 g, 8.12 mmol) in thf (200 mL) was then added dropwise via a cannula over an hour, resulting in a pale red solution that was then allowed to warm to room temperature overnight. The resulting off-white suspension was hydrolyzed with H_2O (150 mL) to yield a pale yellow solution, followed by the addition of solid K_2CO_3 with vigorous stirring until the solution took on a turbid appearance. The thf layer was decanted and the remaining solution extracted with CH_2Cl_2. The combined organic fractions were then dried over $MgSO_4$ and taken to dryness on a rotary evaporator. Recrystallization from boiling Me_2CO afforded the tan-colored product (1.36 g, 6.53 mmol, 80.4%). **Method B:** 4,5-diazafluoren-9-one (1.993 g, 10.94 mmol) was dissolved in thf (250 mL) to afford a pale yellow solution. Dropwise and with vigorous stirring, ClMgC≡CH (ca. 0.5 M in thf, 70 mL, 35 mmol) was added over 30 min during which time the solution developed an opaque brown appearance. After being stirred for 4 h the reaction was opened to the atmosphere, diluted with 300 mL of Et_2O, then quenched by slow addition of 400 mL of saturated aqueous NH_4Cl solution. The product was extracted with $CHCl_3$, dried over $MgSO_4$, and taken to dryness by rotary evaporation. The crude reaction product was adsorbed onto SiO_2 (ca. 40 g) and eluted with acetone to yield the pure product after removal of solvent under reduced pressure (2.045 g, 9.821 mmol, 89.8%). Mp >236 °C dec. Anal. Calcd for $C_{13}H_8N_2O_1 \cdot {}^1/_3H_2O$: C, 72.89; H, 4.08; N, 13.08. Found: C, 72.47; H, 4.23; N, 12.97. ^{1}H NMR (500 MHz, $(CD_3)_2CO$): δ (ppm) 8.69 (dd, 2H, H3/H6), 8.14 (dd, 2H, H1/H8), 7.46 (dd, 2H, H2/H7), 5.98 (s, 1H, OH), 3.08 (s, 1H, C≡CH). ^{13}C{^{1}H} NMR (125 MHz, $(CD_3)_2CO$): δ (ppm) 159.5 (C4′/C5′), 152.4 (C3/C6), 145.5 (C1′/C8′), 133.7 (C1/C8), 125.6 (C2/C7), 85.8 (*C*≡CH), 74.5 (C≡*C*H), 72.8 (C9). IR (cm^{-1}): υ_{water} 3542 m, υ_{OH} and $\upsilon_{C\equiv CH}$ 3259 s, 3235 s, 3104 (br) m, $\upsilon_{C\equiv C}$ 2102 w. EI-MS (Me_2CO): *m*/*z* 208 [100%, M^+]. UV–vis (MeCN) λ (nm) [$\epsilon \times 10^4$ M^{-1} cm^{-1}]: 226 [1.00], 266 [0.787], 304 [1.52], 314 [1.93].

Syntheses of Allenylidene Complexes 2–5. The syntheses, isolation, and purification of complexes **3** to **5** are analogous to the procedure described in detail for **2** below. The numbering scheme utilized in NMR resonance assignments is outlined in Figure 1.

Complex 2, [RuCl(dppm)$_2$=C=C=(4,5-diazafluoren-9-yl)]-PF_6. *cis*-[$RuCl_2$(dppm)$_2$] (944 mg, 1.00 mmol), **1** (225 mg, 1.08 mmol), and $NaPF_6$ (280 mg, 1.67 mmol) were combined in a Schlenk flask and stirred in vacuo for approximately an hour before the addition of CH_2Cl_2 (140 mL). The solution was stirred at room temperature for ca. 50 h, then opened to the atmosphere, filtered through celite, and taken to dryness under reduced pressure. The crude product was crystallized from CH_2Cl_2/EtOH, washed successively with cold EtOH and Et_2O, and air-dried to yield the

(17) Herndon, J. W. *Coord. Chem. Rev.* **1999**, *181*, 177.
(18) Herndon, J. W. *Coord. Chem. Rev.* **2000**, *209*, 387.
(19) Herndon, J. W. *Coord. Chem. Rev.* **2001**, *214*, 215.
(20) Herndon, J. W. *Coord. Chem. Rev.* **2002**, *227* (1), 1.
(21) Herndon, J. W. *Coord. Chem. Rev.* **2003**, *243* (1–2), 3.
(22) Herndon, J. W. *Coord. Chem. Rev.* **2004**, *248,* (1–2), 3.
(23) Bruce, M. I. *Chem. Rev.* **1998**, *98*, 2797.
(24) Cadierno, V.; Gamasa, M. P.; Gimeno, J. *Eur. J. Inorg. Chem.* **2001**, 571.
(25) Bruce, M. I.; Low, P. J. *Adv. Organomet. Chem.* **2004**, *50*, 179.
(26) Touchard, D.; Dixneuf, P. H. *Coord. Chem. Rev.* **1998**, *409*, 178–180.
(27) Werner, H.; Ilg, K.; Lass, R.; Wolf, J. *J. Organomet. Chem.* **2002**, *661*, 137.
(28) Werner, H. *Chem. Commun.* **1997**, 903.
(29) Selegue, J. P. *Organometallics* **1982**, *1*, 217.
(30) Berke, H. *Angew. Chem., Int. Ed. Engl.* **1976**, *15*, 624.
(31) Plater, M. J.; Kemp, S.; Lattmann, E. *J. Chem. Soc., Perkin Trans. 1* **2000**, 971.
(32) Chaudret, B.; Commenges, G.; Poilblanc, R. *J. Chem. Soc., Dalton Trans.* **1984**, 1635.
(33) Armarego, W. L. F.; Chai, C. L. L. *Purification of Laboratory Chemicals*, 5th ed.; Butterworth-Heinemann: Burlington, MA, 2003.
(34) Midland, M. M. *J. Org. Chem.* **1975**, *40*, 2250.

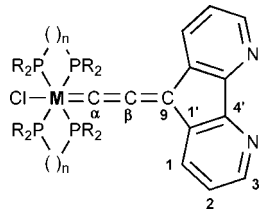

Figure 1. Atom labeling scheme utilized in assignment of NMR spectroscopic data.

product as a red-brown powder (1.042 g, 0.841 mmol, 83.7%). Analytically pure samples were obtained by silica chromatography, preadsorbing the compound onto silica gel and eluting with a 2% saturated solution of KPF_6 in MeCN, collecting the maroon fraction. This column fraction was taken to dryness under reduced pressure, redissolved in CH_2Cl_2, washed copiously with water, dried over $CaSO_4$, then recrystallized from CH_2Cl_2/EtOH to yield maroon-red crystals. Anal. Calcd for $C_{63}H_{50}ClF_6N_2P_5Ru_1$: C, 60.99; H, 4.06; N, 2.26. Found: C, 61.28; H, 3.84; N, 2.45. ^{1}H NMR (600 MHz, $(CD_3)_2CO$): δ (ppm) 8.74 (dd, 2H, H3), 7.69–7.63 (m, 8H, phenyl), 7.43–7.39 (m, 4H, phenyl), 7.39–7.35 (m, 8H, phenyl), 7.33–7.26 (m, 12H, phenyl), 7.22–7.17 (m, 8H, phenyl), 6.84 (dd, 2H, H2), 5.89 (m, 2H, PCH_2P), 5.72 (m, 2H, PCH_2P), 5.54 (dd, 2H, H1). $^{13}C\{^1H\}$ NMR (125 MHz, $(CD_3)_2CO$): δ (ppm) 324.6 (quintuplet, Cα), 241.1 (m, Cβ), 164.1 (s, C4′), 152.6 (s, C3), 146.8 (s, C9), 135.9 (s, C1′), 131.0 (s, C1), 125.0 (s, C2), 42.5 (quintuplet, PCH_2P), 133.8 and 133.6 (quintuplet, C_{ortho}), 132.4 and 131.8 (s, C_{para}), 131.7 and 130.4 (quintuplet, C_{ipso}), 130.2 and 129.4 (t, C_{meta}). $^{31}P\{^1H\}$ NMR (202 MHz, $(CD_3)_2CO$): δ (ppm) –15.16 (s, *trans*-dppm), –142.66 (septet, PF_6^-). IR (cm^{-1}): $\upsilon_{C=C=C}$ 1927 (s), $\upsilon_{PF_6^-}$ 838 (vs). FAB-MS (CH_2Cl_2): *m*/*z* 1095 [100%, M^+]. UV–vis (MeCN) λ (nm) [$\epsilon \times 10^4$ M^{-1} cm^{-1}]: 232 [5.98], 274 [5.46], 454_{sh} [1.59], 510 [1.65].

Complex 3, [RuCl(dppe)$_2$=C=C=(4,5-diazafluoren-9-yl)]-PF$_6$. *cis*-[$RuCl_2$(dppe)$_2$] (483 mg, 0.498 mmol), **1** (118 mg, 0.521 mmol), and $NaPF_6$ (143 mg) were refluxed for 3 days in 1,2-dichloroethane (125 mL). Workup and recrystallization yielded the deep maroon product as microcrystals (324 mg, 0.255 mmol, 51.5%). Anal. Calcd for $C_{65}H_{54}Cl_1F_6N_2P_5Ru_1 \cdot {}^1/_2CH_2Cl_2$: C, 60.00; H, 4.23; N, 2.14. Found: C, 60.47; H, 4.20; N, 2.34. ^{1}H NMR (500 MHz, $(CD_3)_2CO$): δ (ppm) 8.83 (d, 2H, H3), 7.40 (t, 4H, phenyl), 7.29–7.23 (m, 8H, phenyl), 7.22–7.13 (m, 12H, phenyl), 7.03–6.96 (m, 18H, H2 and phenyl), 6.58 (d, 2H, H1), 3.47–3.27 (m, 8H, $P(CH_2)_2P$). $^{13}C\{^1H\}$ NMR (125 MHz, $(CD_3)_2CO$): δ (ppm) 321.83 (quintuplet, Cα), 248.46 (m, Cβ), 164.53 (s, C4′), 152.80 (s, C3), 149.14 (s, C9), 136.79 (s, C1′), 130.11 (s, C1), 125.66 (s, C2), 29.23 (quintuplet, $P(CH_2)_2P$), 134.77, 133.71, 132.10, 131.79, 129.76, 129.04 (s, C_{ortho}, C_{meta}, C_{para}), 133.04 and 132.57 (m, C_{ipso}). $^{31}P\{^1H\}$ NMR (202 MHz, $(CD_3)_2CO$): δ (ppm) 36.71 (s, *trans*-dppe), –142.65 (septet, PF_6^-). IR (cm^{-1}): $\upsilon_{C=C=C}$ 1909 (s), $\upsilon_{PF_6^-}$ 840 (vs). FAB-MS (CH_2Cl_2): *m*/*z* 1123 [100%, M^+]. UV–vis (MeCN) λ (nm) [$\epsilon \times 10^4$ M^{-1} cm^{-1}]: 230 [5.907], 274 [5.897], 452 [1.572] 532 [1.386].

Complex 4, [RuCl(dmpe)$_2$=C=C=(4,5-diazafluoren-9-yl)]-PF$_6$. [$RuCl_2$(dmpe)$_2$] (262 mg, 0.554 mmol), **1** (102 mg, 0.490 mmol), and $NaPF_6$ (102 mg) were refluxed for 4 days in 1,2-dichloroethane (100 mL). Solvent was removed in vacuo and the residue was recrystallized from 2:1 CH_2Cl_2:Et_2O (25 mL) to yield **4** as a deep maroon powder (240 mg, 0.311 mmol, 63.4%). Rapid decomposition in solution prevented satisfactory purification and full characterization. Anal. Calcd for $C_{25}H_{38}Cl_1F_6N_2P_5Ru_1$: C, 38.90; H, 4.96; N, 3.63. Found: C, 37.84; H, 5.38; N, 2.51. $^{31}P\{^1H\}$ NMR (202 MHz, CD_2Cl_2): δ (ppm) 31.1 (s, *trans*-dmpe), –143.85 (septet, PF_6^-). IR (cm^{-1}): $\upsilon_{C=C=C}$ 1910 (m), $\upsilon_{PF_6^-}$ 843 (s). FAB-MS (CH_2Cl_2): *m*/*z* 627 [16.8%, M^+].

Complex 5, [OsCl(dppm)$_2$=C=C=(4,5-diazafluoren-9-yl)]-PF$_6$. [$OsCl_2$(dppm)$_2$] (65 mg, 0.063 mmol), **1** (14 mg, 0.062 mmol), and $NaPF_6$ (13 mg, 0.076 mmol) were refluxed overnight in 1,2-dichloroethane (25 mL). Workup and recrystallization yielded the product as a deep orange-red powder (51 mg, 0.038 mmol, 62%). Anal. Calcd for $C_{63}H_{50}Cl_1F_6N_2Os_1P_5$: C, 56.91; H, 3.79; N, 2.11. Found: C, 56.30; H, 3.93; N, 2.46. ^{1}H NMR (500 MHz, CD_2Cl_2): δ (ppm) 8.99 (dd, 2H, H3), 7.42 (t, 4H, phenyl), 7.33–7.31 (br m, 8H, phenyl), 7.27–7.16 (m, 28H, phenyl), 6.78 (dd, 2H, H2), 6.28 (dt, 2H, PCH_2P), 5.82 (dt, 2H, PCH_2P), 5.79 (dd, 2H, H1). $^{13}C\{^1H\}$ NMR (125 MHz, CD_2Cl_2): δ (ppm) 280.8 (quintuplet, Cα), 255.6 (m, Cβ), 163.32 (s, C4′), 151.7 (s, C3), 141.75 (s, C1′), 140.98 (s, C9), 129.88 (s, C1), 124.83 (s, C2), 49.1 (quintuplet, PCH_2P), 133.05, 132.56, 132.10, 131.66, 129.48, 128.91 (s, C_{ortho}, C_{meta}, C_{para}), 129.67 (m, C_{ipso}). $^{31}P\{^1H\}$ NMR (202 MHz, CD_2Cl_2): δ (ppm) –60.92 (s, *trans*-dppm), –143.85 (septet, PF_6^-). IR (cm^{-1}): $\upsilon_{C=C=C}$ 1927 (s), $\upsilon_{PF_6^-}$ 850 (vs). FAB-MS (CH_2Cl_2): *m*/*z* 1184 [100%, M^+]. UV–vis (MeCN) λ (nm) [$\epsilon \times 10^4$ M^{-1} cm^{-1}]: 232 [7.226], 252 [6.517], 438_{sh} [1.853], 472 [2.214].

Electrochemical/Spectroelectrochemical Experiments. Cyclic voltammetry measurements were performed on an ADInstruments Maclab/4e interface and Maclab potentiostat (1 mm diameter Pt disk working, Pt auxiliary and Ag/AgCl reference mini-electrode). Solutions contained 0.1 M [^{n}Bu$_4$N]PF_6 and 5–10 mM complex in CH_2Cl_2, purged and maintained under an atmosphere of argon (0.25 M [^{n}Bu$_4$N]PF_6 and ca. 1 mM complex, under nitrogen, for spectroelectrochemical experiments). Scan rates were 100 mV s^{-1} and referenced to the internal FcH/FcH^+ couple ($E^0 = 0.56$ V, $\Delta E_p = 0.07$ V). Spectroelectrochemical data were recorded on a Cary 5 spectrophotometer (45000−4000 cm^{-1}) in CH_2Cl_2. Solution UV–vis spectra of the reduced species at −35 °C were obtained by electrogeneration (Thompson 401E potentiostat) at a Pt gauze working electrode within a cryostated, optically transparent, thin-layer electrochemical (OTTLE) cell, path length 0.5 mm, under an atmosphere of nitrogen.[35] The efficiency and reversibility of each step was tested by applying a sufficiently positive potential to oxidize the product; stable isosbestic points were observed in the spectral progressions for all the transformations reported herein.

Structure Determinations. Full spheres of CCD area-detector diffractometer data were measured (ω-scans; monochromatic Mo Kα radiation, $\lambda = 0.7107_3$ Å (exception: **3** for which a synchrotron source was used, $\lambda = 0.4859_5$ Å), yielding $N_{t(otal)}$ reflections, these merging to N unique (R_{int} cited) after "empirical"/multiscan absorption correction (proprietary software), N_o with $I > 2\sigma(I)$ considered "observed"). All reflections were used in the full-matrix least-squares refinements on F^2, refining anisotropic displacement parameter forms for the non-hydrogen atoms (exceptions: **3**, **4** Ru, Cl, P only anisotropic), hydrogen atom treatment following a riding model (reflection weights: $(\sigma^2(F_o^2) + (aP)^2 + (bP)^{-1}$ ($P = (F_o^2 + 2F_c^2)/3$)). Neutral atom complex scattering factors were employed within the SHELXL 97 program.[36] Pertinent results are given in the text, tables, and figures, the latter showing non-hydrogen atoms with 20% (room temperature) or 50% ('low' temperature) probability amplitude displacement envelopes, hydrogen atoms having an arbitrary radius of 0.1 Å. Individual diversions in procedure are noted in the footnotes to Table 1.

Theoretical Methods. Density functional theory calculations were executed in this study using the Amsterdam Density Functional

(35) Duff, C. M.; Heath, G. A. *Inorg. Chem.* **1991**, *30*, 2528.
(36) Sheldrick, G. M. *SHELX-97; A program for crystal structure refinement*; University of Goettingen: Goettingen, Germany, 1997.

Table 1. Crystal Data and Refinement Details for 1–5

	1 · ½H_2O[a]	**2**[PF_6][b]	**3**[PF_6] · $^1/_{16}H_2O$[c]	**4**[PF_6] · $^1/_4Et_2O$ · $^1/_2CH_2Cl_2$[d]	**5**[PF_6][b]
formula	$C_{13}H_9N_2O_{1.5}$	$C_{63}H_{50}ClF_6N_2P_5Ru$	$C_{65}H_{54.125}ClF_6N_2O_{0.0625}P_5Ru$	$C_{26.5}H_{41.5}Cl_2F_6N_2O_{0.25}P_5Ru$	$C_{63}H_{50}ClF_6N_2P_5Os$
M_r	217.2	1240.5	1270.5	832.9	1329.6
cryst system	orthorhombic	orthorhombic	triclinic	monoclinic	orthorhombic
space group	*Pbca* (no. 61)	*Pnma* (no. 62)	$P\bar{1}$(no. 2)	$P2_1$ (no. 4)	*Pnma* (no. 62)
a (Å)	12.113(1)	17.950(2)	22.985(1)	16.916(3)	17.9908(7)
b (Å)	11.944(1)	17.876(2)	24.367(2)	25.381(4)	17.8767(8)
c (Å)	29.432(3)	17.543(2)	41.672(1)	17.050(3)	17.6251(7)
V (Å^3)	4258	5629	23127	7044	5669
D_c (g cm^{-3})	1.35_5	1.46_4	1.46_0	1.57_1	1.55_8
Z (fu)	16	4	16	8	4
μ_{Mo} (mm^{-1})	0.091	0.53	0.28	0.88	2.5
specimen (mm^3)	0.72 × 0.48 × 0.11	0.41 × 0.17 × 0.15	0.08 × 0.06 × 0.02	0.14 × 0.07 × 0.06	0.30 × 0.20 × 0.06
$T_{min/max}$	0.81	0.66	0.81	0.82	0.74
$2\theta_{max}$ (deg)	58	55	34	45	75
N_t	17718	63326	338361	54714	117225
N (R_{int})	4852 (0.052)	6723 (0.12)	79947 (0.091)	18063 (0.099)	15015 (0.041)
N_o	2747	3789	53384	13640	11566
*R*1	0.043	0.069	0.072	0.097	0.027
*wR*2	0.100	0.20	0.19	0.24	0.067
a, *b*	0.0449	0.1072	0.0905, 62.3	0.0837, 94.5	0.0353
S	0.98	1.06	1.04	1.05	1.05
T (K)	ca. 298	ca. 153	ca. 103	ca. 153	ca. 153

[a] Water molecule hydrogen atoms were refined in (*x*, *y*, *z*, U_{iso}). [b] **2** and **5** are isomorphous. [c] α, β, and γ were 83.66(3)°, 89.79(3)°, and 85.56(3)°; in complex **4**, the central PCCP string and a pendant phenyl at either end were modeled as disordered over pairs of sites, occupancies refining to 0.65(1) and complement (component/"molecule 9"). [d] β was 105.780(3)°.

(ADF) program, version ADF 2004.01,[37] developed by Baerends et al.[38,39] Calculations were variously performed on Linux-based Pentium IV 2.8 GHz computers, or in parallel mode on the AlphaServer supercomputer housed at the ANU Supercomputer Facility and operated under the Australian Partnership for Advanced Computing. Calculations were variously performed in C_1 and in C_{2v} symmetry. Electrons in orbitals up to and including 1s {C, N}, 2p {P, Cl}, and 4d {Ru} were treated in accordance with the frozen-core approximation. Geometry optimizations employed the gradient algorithm of Versluis and Ziegler.[40] Functionals used in the calculations were the local density approximation (LDA) to the exchange potential,[41] the correlation potential of Vosko, Wilk, and Nusair (VWN),[42] and the nonlocal corrections of Perdew, Burke, and Enzerhof (PBE).[43] In all calculations, the (Slater type orbital) basis sets used were of triple-ζ-plus-polarization quality (TZP) for "central" atoms (i.e., Ru, P, Cl, N, and the three allenylidene C atoms) and of double-ζ quality (DZ) for "peripheral" atoms (i.e., other C atoms, and H). Calculations were pursued both in the vacuum phase ($\epsilon = 1$) and with solvent corrections, which were applied using the COSMO (COnductor-like Screening MOdel) protocol,[44–46] for dielectric constant values of $\epsilon = 4$ and 10.

Scheme 1. Synthesis of 9-Hydroxy-9-Ethynyl-4,5-Diazafluorene (1) from 4,5-Diazafluoren-9-one[a]

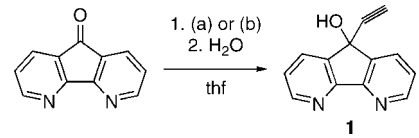

1

[a] Conditions: (a) LiC≡CH, −78 °C; (b) ClMgC≡CH, rt.

Results and Discussion

Synthesis and Characterization of 9-Hydroxy-9-ethynyl-4,5-diazafluorene, 1. From the ketone precursor 4,5-diazafluoren-9-one, the alkynol **1** is readily accessed in high yield via nucleophilic attack with either lithium acetylide[34] or ethynylmagnesium chloride and subsequent hydrolysis (Scheme 1). All ^1H and ^{13}C NMR spectroscopic resonances were unambiguously assigned utilizing the $^1H-^{13}C$ HSQC and HMBC NMR techniques, and all data were found to be consistent with expectations. The $\upsilon_{C\equiv C}$ resonance is clearly identified in the infrared spectrum at 2102 cm^{-1}, while assignment of the frequencies attributable to $\upsilon_{C\equiv C-H}$ and υ_{OH} is confused by differences in H-bonding motifs within the molecule. In the crystal structure of **1**, two independent molecules devoid of crystallographic symmetry, accompanied by a single water molecule, make up the asymmetric unit of the structure. The hydroxyl group of molecule-1 hydrogen bonds to the water-molecule oxygen atom (O,H(13)···O(01) 2.693(2), 1.8_8 Å (est.)), the water molecule, in turn, hydrogen bonding to a nitrogen atom of molecule-2 (O(01),H(01B)···N(21) 2.870(2), 2.0_2 Å (est.)) and the hydroxyl oxygen atom of a different molecule-2 (O(01),H(01A)···O(23) (2 − *x*, 2 − *y*, 1 − *z*) 3.011(2), 2.2_0 Å (est.)) (Figure 2a), resulting, at the supramolecular level, in a structure layered normal to *c* (Figure 2b).

(37) Baerends, E. J.; Autsbach, J.; Bérces, A.; Bo, C.; Boerrigter, P. M.; Cavallo, L.; Chong, D. P.; Deng, L.; Dickson, R. M.; Ellis, D. E.; Fan, L.; Fischer, T. H.; Fonseca Guerra, C.; van Gisbergen, S. J. A.; Groeneveld, J. A.; Gritsenko, O. V.; Gruning, M.; Harris, F. E.; van den Hoek, P.; Jacobsen, H.; van Kessel, G.; Kootstra, F.; van Lenthe, E.; McCormack, D. A.; Osinga, V. P.; Patchkovskii, S.; Philipsen, P. H. T.; Post, D.; Pye, C.; Ravenek, W.; Ros, P.; Schipper, P. R. T.; Schreckenbach, G.; Snijders, J. G.; Sola, M.; Swart, M.; Swerhone, D.; te Velde, G.; Vernooijs, P.; Versluis, L.; Visser, O.; van Wezenbeek, E.; Wiesenekker, G.; Wolff, S. K.; Woo, T. K.; Ziegler, T. *ADF2004.01, S.C.M.*; Theoretical Chemistry, Vrije Universiteit: Amsterdam, The Netherlands, 2004; http://www.scm.com.

(38) Fonseca Guerra, C. F.; Snijders, J. G.; te Velde, G.; Baerends, E. J. *Theor. Chem. Acc.* **1998**, *99*, 391.

(39) te Velde, G.; Bickelhaupt, F. M.; Baerends, E. J.; Fonseca Guerra, C. F.; van Gisbergen, S. J. A.; Snijders, J. G.; Ziegler, T. *J. Comput. Chem.* **2001**, *22*, 931.

(40) Versluis, L.; Ziegler, T. *J. Chem. Phys.* **1988**, *88*, 322.

(41) Parr, R. G.; Yang, W. *Density Functional Theory of Atoms and Molecules*; Oxford University Press: New York, 1989.

(42) Vosko, S. H.; Wilk, L.; Nusair, M. *Can. J. Chem.* **1980**, *58*, 1200.

(43) Perdew, J. P.; Burke, K.; Ernzerhof, M. *Phys. Rev. Lett.* **1996**, *77*, 3865.

(44) Klamt, A. *J. Phys. Chem.* **1995**, *99*, 2224.

(45) Klamt, A.; Schüürmann; G, J. *J. Chem. Soc., Perkin Trans. 2* **1993**, 799.

(46) Pascual-Ahuir, J. L.; Silla, E.; Tomasi, J.; Bonaccorsi, R. *J. Comput. Chem.* **1987**, *8*, 778.

(47) Madhavi, N. N. L.; Bilton, C.; Howard, J. A. K.; Allen, F. H.; Nangia, A.; Desiraju, G. R. *New J. Chem.* **2000**, *24*, 1.

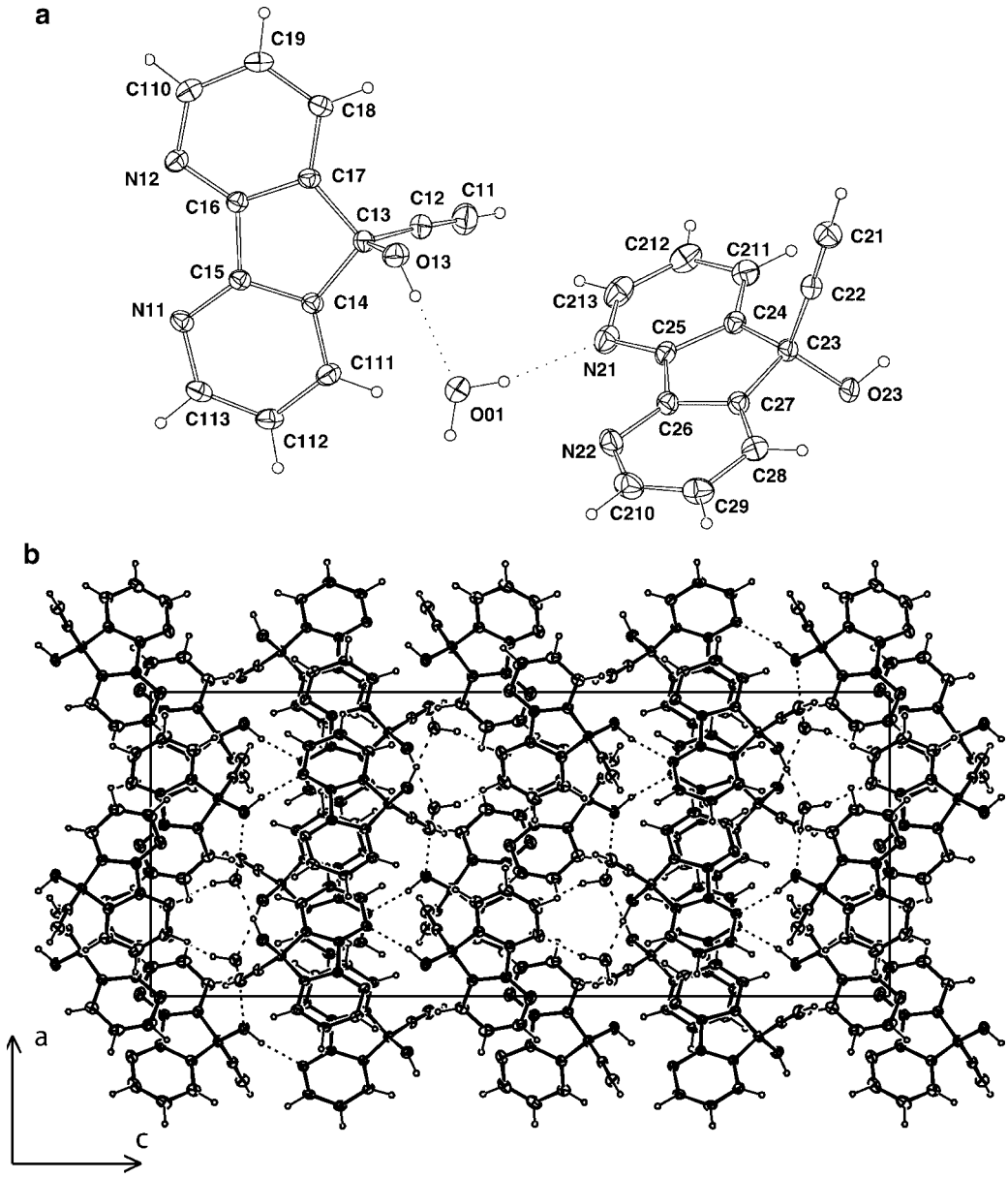

Figure 2. (a) The two independent molecules of the asymmetric unit of **1** showing hydrogen-bonding interactions with the accompanying water molecule. (b) Unit cell contents projected down *b*, showing the supramolecular layers normal to *c* linked by hydrogen bonds.

Scheme 2. Synthesis and Numbering of the Allenylidene Complexes

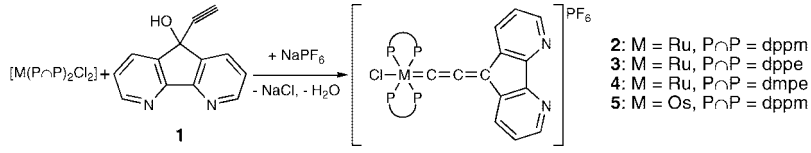

Bond lengths and angles are much as expected, the triple bonds C(n1)−C(n2) being strongly localized (1.168(3), 1.179(2) Å, cf. C(n2)−C(n3) 1.479(2), 1.483(2) Å); C(n1)−C(n2)−C(n3) 175.9(2), 176.5(2)°; the closest contact to an alkynyl hydrogen atom is C,H(21)···O(23) ($1.5 - x$, $y - ½$, z) 3.497(2), 2.6_8 Å (est.), in preference to the possibility of CH-π interactions often evident in analogous alkynol compounds.[47]

Synthesis of Bis(diphosphine) Allenylidene Complexes 2–5 Bearing the Terminal Diazafluorenyl Moiety. Following the procedure first introduced by Selegue in 1982,[29] the allenylidene complexes **2**–**5** are prepared by reaction of the propargylic alcohol **1** with the respective bis(diphosphine) metal complexes. Abstraction of a chloride from $MCl_2(P∩P)_2$ utilizing $NaPF_6$ leads to a coordinatively unsaturated 16-electron intermediate $[MCl(P∩P)_2](PF_6)$, which reacts with the alkyne functionality of **1** and through dehydration gives the allenylidene complex (Scheme 2).

Reaction of *cis*-$[RuCl_2(dppm)_2]$ and *cis*-$[OsCl_2(dppm)_2]$ with $NaPF_6$ is rapid at room temperature in dichloromethane or 1,2-dichloroethane, the intense and characteristic color change resulting from formation of the $[MCl(dppm)_2]^+$ intermediate noticeable instantly on addition of solvent to the combined dry reactants. Chloride abstraction from $[RuCl_2(dppe)_2]$ and $[RuCl_2(dmpe)_2]$ does not proceed under analogous conditions, however, requiring elevated temperatures such as those afforded

by refluxing 1,2-dichloroethane before any change is evident. In particular it must be noted that $NaPF_6$ is unable to affect halide abstraction from *trans*-$[RuCl_2(dppe)_2]$,[48] and it is consequently imperative to ensure that the starting material is pure *cis*-isomer.

Reaction products were invariably contaminated with impurities tentatively attributable to decomposition of the $[MCl(P\cap P)_2]^+$ intermediate and/or the allenylidene complex, identified by spectroscopy. Though the reactivity of the allenyl moiety in allenylidene complexes is well-established, characterized by nucleophilic attack at the Cα and Cγ carbons and electrophilic attack at the Cβ carbon,[23,49–51] decomposition products of allenylidene complexes are not described nor characterized. Water has been reported to oxidatively cleave the Cα=Cβ bond of allenylidene complexes to form a carbonyl complex and the respective organic alkene,[52–54] while a similar reaction may be postulated with molecular oxygen to afford the carbonyl complex and a ketene.

The reaction of **1** with metal head-groups such as RuCl(Cp)-$(PPh_3)_2$ or $[RuCl_2(p\text{-cymene})]_2$ results in complications due to bipyridyl-like coordination in preference to allenylidene formation,[55,56] and, although the coordination sphere of the bis(diphosphine) metal complexes is comparatively more inert to substitution, it is conceivable that a competitive κ-N vs η-C≡C process is a source of disruption to the mechanism of allenylidene formation.

Crude reaction mixtures in the synthesis of the $[RuCl(dmpe)_2]^+$-derived allenylidene complex **4** were contaminated with numerous compounds that were not isolated, the high reactivity of the complex hindering purification for full analytical and spectroscopic characterization. It remains a challenge to determine an efficient and clean synthesis of this particular complex.

Spectroscopic Characterization of the Allenylidene Complexes. The expected *trans*-octahedral configurations of the chloride and allenylidene ligands at the metal centers are confirmed by the observation of sharp singlet resonances in the ^{31}P NMR spectra of all compounds, the chemical shifts of which are consistent with those of related allenylidene complexes. Mention must be made of the fact that ^{31}P NMR resonances of these allenylidene complexes lie within only a few ppm of the corresponding *trans*-$[MCl(P\cap P)_2(CO)]^+$ species,[57,58] consistent with previous observations about the similar π-acidity of allenylidene and carbonyl ligands.[23] The analysis of ^{13}C NMR spectroscopic data for compounds **2**, **3**, and **5** is consistent with results obtained for other bis(diphosphine) allenylidene complexes exhibiting characteristic low-field Cα resonances around

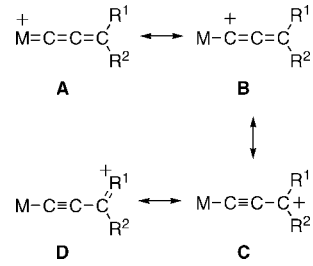

Figure 3. Possible mesomer forms for a cationic allenylidene complex.

320 ppm for Ru[23,49–51] and 280 ppm for Os,[59,60] with the Cβ and Cγ resonances, distinguished by $^nJ_{P,C}$ and $^1H-^{13}C$ HMBC experiments, at progressively higher field. The remainder of the carbon resonances attributable to the diazafluorenyl moiety were distinguished through $^1H-^{13}C$ HSQC and HMBC NMR experiments. There are two sets of resonances of equal intensity for each of the four chemically nonequivalent carbon atoms of the phosphanyl rings, logically attributable to the different environment of those phenyl rings facing the chloride or allenylidene apex of the phosphine−ligand plane, though it was not possible to completely differentiate one set from the other.

Very notable and characteristic spectroscopic features of the compounds are the ^1H NMR resonances of both the diazafluorenyl and phosphine−ligand protons. Interactions between protons at the 1-position of the diazafluorenyl moiety and ring-currents of the "overhanging" phosphanyl phenyl rings lead to a significant shielding effect of between 1.56 and 2.60 ppm from the free ligand. Protons at the 2-position are also shielded by 0.46–0.68 ppm, while those at the 3-position (α to nitrogen) are marginally *de*shielded. The nonequivalent phenyl rings to either side of the phosphine ligand plane also show separate proton (and carbon) resonances, though confident assignment is again not possible due to the partial overlap of certain resonances. In the case of the dppm-ligated complexes **2** and **5**, the two bridging methylene protons also show distinct resonances with significantly different $^nJ_{H,P}$ values, while the bridging ethylene group in compound **3** does not resolve beyond a complex multiplet. Variable-temperature ^1H NMR experiments were undertaken but did not yield sufficient information to further resolve individual resonances.

The characteristic $\upsilon_{C=C=C}$ absorption of group VIII allenylidene complexes lies between 2000 and 1900 cm^{-1}, analogous to that of free allenes H_2C=C=CR_2 (~1950 cm^{-1})[61] and intermediate between those of σ-alkynyl (2140–2040 cm^{-1})[62] and vinylidene (1650–1600 cm^{-1})[63] complexes. Complexes **2–5** absorb at fairly low energy between 1909 and 1927 cm^{-1}, consistent with analogous aryl-substituted allenylidene complexes (e.g., $RuCl(dppe)_2C$=C=CPh_2, 1923 cm^{-1}; $RuCl(dppm)_2$-C=C=CR_2, R_2 = Ph_2 1927 cm^{-1}, R_2 = fluoren-9-yl 1939 cm^{-1}).[64,65] The energy of this vibration provides some insight into the bonding mode of the allenyl moiety (see Figure 3

(48) Chin, B.; Lough, A. J.; Morris, R. H.; Schweitzer, C. T.; D'Agostino, C. *Inorg. Chem.* **1994**, *33*, 6278.
(49) Cadierno, V.; Gamasa, M. P.; Gimeno, J. *Eur. J. Inorg. Chem.* **2001**, *3*, 571.
(50) Rigaut, S.; Touchard, D.; Dixneuf, P. H. *Coord. Chem. Rev.* **2004**, *248* (15–16), 1585.
(51) Winter, R. F.; Zalis, S. *Coord. Chem. Rev.* **2004**, *248*, 1565.
(52) Bianchini, C.; de los Rios, I.; Lopez, C.; Peruzzini, M.; Romerosa, A. *J. Organomet. Chem.* **2000**, *485*, 593–594.
(53) Bianchini, C.; Peruzzini, M.; Zanobini, F.; Lopez, C.; de los Rios, I.; Romerosa, A. *Chem. Commun.* **1999**, 443.
(54) Datta, S.; Chang, C.-L.; Yeh, K.-L.; Liu, R.-S. *J. Am. Chem. Soc.* **2003**, *125*, 9294.
(55) Sanford, V. Hons. Thesis, University of Western Australia, Perth, 1998. Hons.
(56) Schauer, P. A. Hons. Thesis, University of Western Australia, Perth, 2003. Hons.
(57) Smith, G.; Cole-Hamilton, D. J. *J. Chem. Soc., Dalton Trans.* **1984**, *6*, 1203.
(58) Smith, G.; Cole-Hamilton, D. J.; Thornton-Pett, M.; Hursthouse, M. B. *J. Chem. Soc., Dalton Trans.* **1985**, *2*, 387.
(59) Colbert, M. C. B.; Lewis, J.; Long, N. J.; Raithby, P. R.; Younus, M.; White, A. J. P.; Williams, D. J.; Payne, N. J.; Yellowlees, L.; Beljonne, D.; Chawdhury, N.; Friend, R. H. *Organometallics* **1998**, *17*, 3034.
(60) Wong, C.-Y.; Che, C.-M.; Chan, M. C. W.; Leung, K.-H.; Phillips, D. L.; Zhu, N. *J. Am. Chem. Soc.* **2004**, *126*, 2501.
(61) Taylor, D. R. *Chem. Rev.* **1967**, *67*, 317.
(62) Manna, J.; John, K. D.; Hopkins, M. D. *Adv. Organomet. Chem.* **1995**, *38*, 79.
(63) Puerta, M. C.; Valerga, P. *Coord. Chem. Rev.* **1999**, *977*, 193.
(64) Touchard, D.; Guesmi, S.; Bouchaib, M.; Haquette, P.; Daridor, A.; Dixneuf, P. H. *Organometallics* **1996**, *15*, 2579.
(65) Touchard, D.; Pirio, N.; Dixneuf, P. H. *Organometallics* **1995**, *14*, 4920.

Table 2. Selected Data for All Structurally Characterized Bis(diphosphine) Ruthenium Allenylidene Complexes [M=C=C=CR^{1}R^2]X

[M]=C=C=CR^{1}R^2]X				distances (Å)				angles (deg)		
[M]	R^1	R^2	X	M=Cα	Cα=Cβ	Cβ=Cγ	M−Cl	Cl−M=Cα	M=Cα=Cβ	Cα=Cβ=Cγ	ref
RuCl(dppm)$_2$	H	Ph	PF_6	1.886(10)	1.254(14)	1.34(2)	2.460(3)	173.4(3)	177.0(8)	174.1(11)	59
	$C_2H_4CH=CH_2$	NMe_2	PF_6	1.950(4)	1.218(6)	1.372(9)	2.4686(10)	175.21(12)	175.3(4)	175.1(6)	68
	3-phenylinden-1-yl^a		PF_6	1.85(2)	1.29(3)	1.39(3)	2.439(6)	175.0(6)	179(2)	177(2)	69, 70
				1.67(2)	1.43(3)	1.42(3)	2.421(5)	176.2(7)	175(1)	172(2)	69, 70
	N(Me)Bz	Me	SbF_6	1.947(6)	1.217(9)	1.398(9)	2.4763(17)	173.35(19)	175.6(6)	170.8(8)	71
	CH_2-(2-Me-3-thienyl)	NMe_2	SbF_6	1.942(9)	1.228(11)	1.405(12)	2.477(2)	171.8(3)	174.1(8)	170.1(11)	72
	Me	Ph	SbF_6	1.894(4)	1.257(6)	1.346(6)	2.456(1)	173.4(1)	171.2(3)	173.9(4)	73
			PF_6	1.896(6)	1.267(8)	1.364(8)	2.454(2)	173.2(2)	171.5(5)	174.8(5)	73
	1-Me-indol-3-yl	Me	SbF_6	1.911(5)	1.245(7)	1.378(7)	2.4790(12)	177.95(15)	179.5(4)	174.7(5)	73
	4,5-diazafluoren-9-yl, **2**		PF_6	1.868(6)	1.255(9)	1.352(9)	2.451(2)	179.9(2)	179.5(6)	178.0(7)	this work
Ru($C_3R^1R^2$)(dppm)$_2$	$CH=CPh_2$	OMe	$(BF_4)_2$	1.997(7)	1.22(1)	1.39(1)	N/A	N/A	175.0(7)	171.4(9)	70
Ru(C≡CPh)(dppe)$_2$	Ph	Ph	PF_6	1.91(1)	1.28(2)	1.35(2)	N/A	N/A	173.9(9)	177(1)	74
RuCl(dppe)$_2$	μ-(1,3-cyclobutadiene)-C≡C-RuCl(dppe)$_2$		PF_6	1.933(3)	1.225(4)	1.372(4)	2.4948(7)	178.49(9)	174.4(2)	178.3(3)	75
	1-butenyl	NMe_2	SbF_6	1.934(8)	1.232(13)	1.393(13)	2.457(2)	176.8(2)	177.8(7)	168.7(9)	76
	C(H)=C(Me)C≡C-RuCl(dppe)$_2$	Me	BF_4	1.923(9)	1.218(12)	1.390(13)	*2.498*	177.3(2)	178.0(8)	178.1(11)	77
	4,5-diazafluoren-9-yl, ***3***^{b}		PF_6	1.875(11)	1.268(7)	1.348(6)	2.467(13)	176.2(12)	177.8(9)	172(3)	this work
RuCl(dmpe)$_2$	4,5-diazafluoren-9-yl, ***4***^{c}		PF_6	1.84(5)	1.28(5)	1.34(4)	2.47(2)	177.5(6)	175(3)	176.5(17)	this work
OsCl(dppm)$_2$	4,5-diazafluoren-9-yl, **5**		PF_6	1.875(2)	1.268(3)	1.343(3)	2.4575(5)	179.92(6)	179.4(2)	177.3(2)	this work

^{a} Two distinct conformers related to the relative orientation of the indenyl ring with respect to the phosphanyl atoms. ^{b} Mean of eight values. ^{c} Mean of four values.

above), the lower energy of the $\upsilon_{C=C=C}$ absorption for these compounds indicating a strong contribution from the cumulenic resonance form **A**, as opposed to higher energy vibrations which are interpreted as corresponding to a greater degree of alkenynyl character **D**.[23,51]

Very few examples of crystallographically characterized bis(diphosphine) allenylidene complexes exist in the literature, as indicated by the structural survey presented in Table 2. A useful consideration in analyzing cumulenylidene complexes is the degree of bond length alternation along the cumulenic chain, allowing further insight into the degree of contribution from the different possible mesomer forms. Those complexes bearing heteroatom substituents at Cγ show significantly greater alternation in Ru═C and C═C bond lengths, reflecting the greater ability of the heteroatom to stabilize charge and hence the alkenynyl resonance form **D**, and consequently it becomes difficult to draw accurate structural correlations to those complexes with a lesser ability to stabilize such a resonance structure. The structural parameters within the allenylidene moiety of complex **2**, particularly the Ru═Cα bond distance, are, however, comparable to those of the RuCl(dppm)$_2$ derived C_3(H)Ph, C_3(Me)Ph, and C_3(3-phenylinden-1-yl) allenylidene complexes (Table 2). Comment on the Ru═Cα bond length in the dppe-derived complex **3** is hindered by the lack of analogous complexes (those characterized bearing either a nonhalide ligand *trans* to the allenylidene or else an additional unsaturated organometallic fragment as a Cγ substituent), although the (mean) Ru═C distance of 1.868(6) Å is well within the accepted parameters for a formal double-bond designation and assignment of allenylidene character. Further comment on the structures of the dmpe-derived ruthenium complex **4** and the osmium dppm complex **5** is also precluded by the lack of direct analogues for which crystallographic information is available, though both metal–carbon bond lengths fall within accepted double-bond values,[23,63,66] and the Cα═Cβ═Cγ bond lengths are consistent with those found in other allenylidene complexes.

Perhaps the most notable structural feature of such bis(diphenylphosphino)-substituted allenylidene complexes is the degree of steric protection afforded to the cumulenic chain by the overhanging phenyl rings. As can be seen in the structure of **2** (Figure 4), the four phenyl rings quasiparallel to the plane of the allenylidene ligand shroud the C_3 allenyl moiety. **2** and **5** are isomorphous, one-half of the molecule comprising the asymmetric unit of each structure, a crystallographic mirror plane containing L, Ru, and Cl and bisecting each dppm ligand

(66) Bruce, M. I. *Chem. Rev.* **1991**, *91*, 197.
(67) Allen, F. H. *Acta Crystallogr.* **2002**, *B58*, 380.
(68) Winter, R. F.; Hornung, F. M. *Organometallics* **1997**, *16*, 4248.
(69) Pirio, N.; Touchard, D.; Toupet, L.; Dixneuf, P. H. *J. Chem. Soc., Chem. Commun.* **1991**, 980.
(70) Touchard, D.; Pirio, N.; Toupet, L.; Fettouhi, M.; Ouahab, L.; Dixneuf, P. H. *Organometallics* **1995**, *14*, 5263.
(71) Winter, R. F.; Hartmann, S.; Zalis, S.; Wilhelm Klinkhammer, K. *Dalton Trans.* **2003**, *11*, 2342.
(72) Harbort, R.-C.; Hartmann, S.; Winter, R. F.; Klinkhammer, K. W. *Organometallics* **2003**, *22*, 3171.
(73) Hartmann, S.; Winter, R. F.; Sarkar, B.; Lissner, F. *Dalton Trans.* **2004**, *20*, 3273.
(74) Touchard, D.; Haquette, P.; Daridor, A.; Romero, A.; Dixneuf, P. H. *Organometallics* **1998**, *17*, 3844.
(75) Rigaut, S.; Le, Pichon, L.; Daran, J.-C.; Touchard, D.; Dixneuf, P. H. *Chem. Commun.* **2001**, 1206.
(76) Winter, R. F.; Klinkhammer, K.-W.; Zalis, S. *Organometallics* **2001**, *20*, 1317.
(77) Rigaut, S.; Massue, J.; Touchard, D.; Fillaut, J.-L.; Golhen, S.; Dixneuf, P. H. *Angew. Chem., Int. Ed.* **2002**, *41*, 4513.
(78) Rigaut, S.; Maury, O.; Touchard, D.; Dixneuf, P. H. *Chem. Commun.* **2001**, 373.

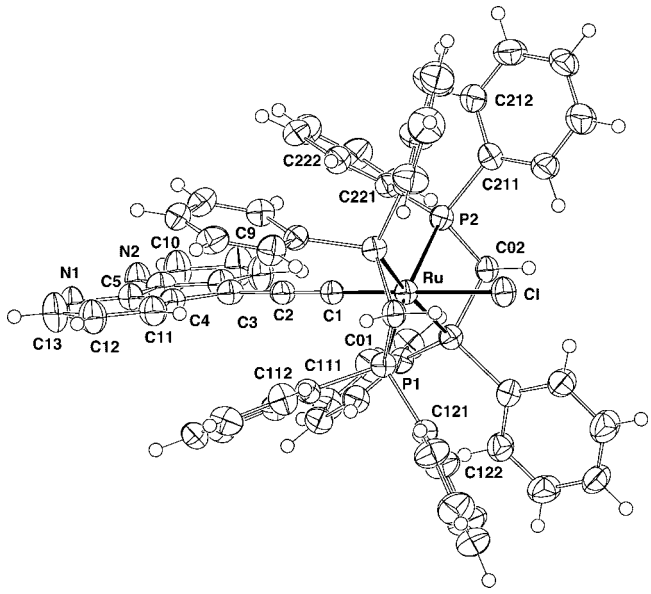

Figure 4. Projection of a single molecule of **2** (**5** is isomorphous), the crystallographic/intramolecular mirror plane lying quasinormal to the page.

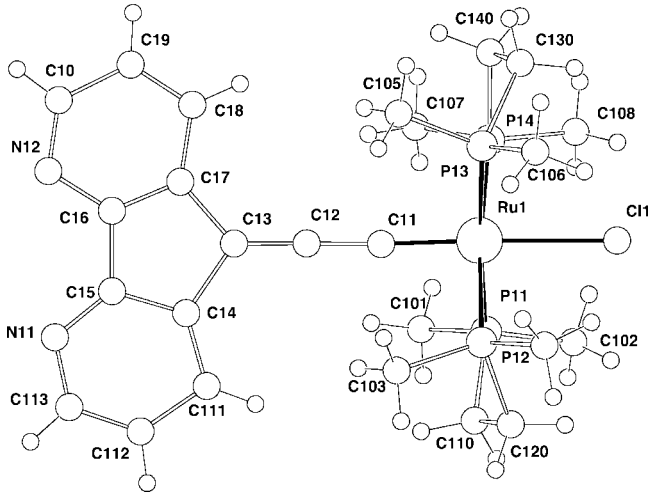

Figure 5. Projection of a single molecule (molecule 1) of **4**, normal to the ligand plane.

at the methylene group. The geometries of the two molecules and the two metal atom environments are very similar, osmium ligand−atom distances perhaps uniformly shorter than their ruthenium counterparts by somewhat less than 0.01 Å (no libration corrections have been applied). The chelate rings of the two dppm ligands are folded similarly so that a pair of methylene C−H bonds lie quasiparallel to and either side of the M−Cl bond.

The structures of **4** (Figure 5) and **3** differ in having a large multiplicity of formula units in the asymmetric unit of each structure: four in **4** and eight in **3**. Both are solvated, the solvent component of **4** being ill-defined and contributing to the imprecision of the determination. Geometries for the molecules of the two compounds are presented in detail in the Supporting Information, presenting mean values of the parameters of the metal atom environments and ligand conformation. One looks in vain for pseudosymmetry, although there are interesting aspects in the crystal packing such as the apparent arrangement of the molecules of **3** in discrete clusters, e.g., in projection down *a* (Figure 6b). More pertinently there are quite significant

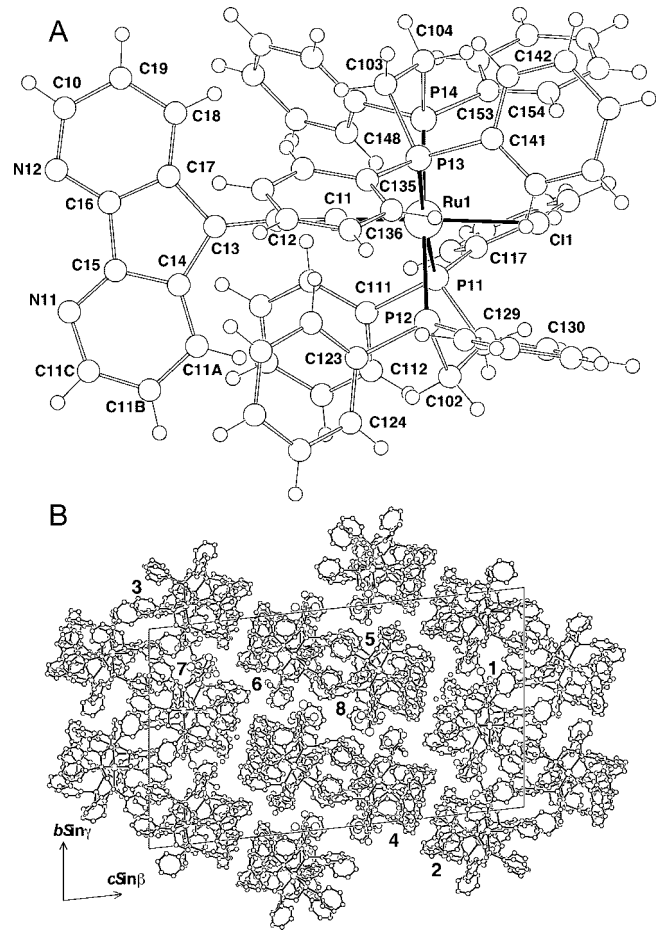

Figure 6. (a) Projection of a single molecule (molecule 1) of **3**, normal to the ligand plane. (b) Unit cell contents projected down *a*, showing the pairwise clustering of the molecules.

differences between the molecules within each of **4** and **3**, suggesting that variations in parameters are real rather than just "noise". Thus, although the precision of the determination of **4** is poor, it suffices to establish that the ligand conformations within three of the molecules of the asymmetric unit are $\lambda\lambda$ in the chirality of the specimen studied, while the fourth is $\lambda\delta$. Despite the large number of molecules in the asymmetric unit of **3** and the (rather minimal) solvation, the use of a synchrotron instrument permits definition of the structure with much better precision, and very considerable differences between the eight molecules of the asymmetric unit can be defined with much greater confidence. Here two of the molecules have $\lambda\delta$ ligand conformations, five are $\lambda\lambda$ (one of these having one disordered ligand), and the sixth $\lambda-$. Ru−Cl distances range over 0.04 Å, Ru=C over ca. 0.03 Å, and Ru−P over nearly 0.1 Å. Among the angular geometries C=Ru−P range between 82.07(6)° and 100.51(6)°, while (e.g.) P−Ru−P(trans) range between 172.20(5)° and 177.07(5)°. Ligand "bite" angles range between 78.66(6)° and 82.40(6)°, those of the $\lambda\delta$ pairs lying toward the upper end of the range.

Electrochemistry and Electronic Spectroscopy. The solution electrochemistry of complexes **2**, **3**, and **5** is defined by two single-electron reductions as summarized in Table 3. The first reduction of the monocation to the neutral species is reversible at room temperature, and theoretical treatments of **2** indicate a ligand-centered process with high spin-densities on the Cα and Cγ atoms accompanied by a marked lengthening of the Ru=Cα and Cβ=Cγ bond lengths and contraction of the Cα=Cβ bond length (Table 4). This is indicative of a change

Table 3. Electrochemical Data (relative to saturated AgCl electrode utilizing FcH/FcH^+ internal standard in CH_2Cl_2 with 0.1 M NBu_4PF_6 supporting electrolyte) and Lowest Energy Uv–Vis Absorbances (in MeCN) of the Allenylidene Complexes

	$E_{1/2}$ (V)		δ [abs]	
	1st	2nd	nm [$\epsilon \times 10^4$ M^{-1} cm^{-1}]	
2	−0.08	−0.95	454 [1.59]	510 [1.65]
3	−0.03	−0.86	452 [1.572]	532 [1.386]
5	−0.25	−1.00	438 [1.853]	472 [2.214]

Table 4. Predicted Vacuum-Phase Structural Parameters of the Electrochemically Generated Species on Reduction of Allenylidene Complex 2

	Ru−Cα	Cα−Cβ	Cβ−Cγ
expt	1.87(1)	1.24(1)	1.35(1)
cation	1.926	1.277	1.349
neutral	1.977	1.251	1.383
anion	2.034	1.241	1.416

in ligand character from cumulenic to acetylenic, and indeed is consistent with related experiments in which such reduced allenylidene species may be trapped and isolated as σ-acetylides through the addition of a hydride source.[78]

The ligand-centered nature of this first reduction is further confirmed experimentally by the UV–vis spectra of the allenylidene complexes. Trends in the $E_{1/2}$ potentials of the first reduction wave follow the energies of the two lowest energy absorptions (ca. 500 nm) in the UV–vis spectra (Table 3), and UV–vis spectroelectrochemical experiments on complex **2** show the disappearance of these paired low-energy absorbances during reduction of the cationic complex to the neutral (see the Supporting Information). Though full assignment of the electronic transitions for the complexes was not possible from theoretical treatments (due to the difficulties discussed below), we hypothesize that these low-energy transitions are an intraligand charge-transfer process that is lost on reduction of the ligand from an allenic to an acetylenic species.

The second reduction process is not reversible at room temperature. However, the spectroelectrochemical experiments on complex **2** indicate that the process *is* reversible at −35 °C. The reduction potentials follow a similar relative trend to the first reduction, and computational results again suggest the process to be entirely ligand centered with a further increase in acetylenic character of the allenylidene ligand. Unfortunately the identity of this anionic, doubly reduced species is not clear from theoretical treatments or the UV–vis spectroelectrochemical experiments.

It is also interesting to note that there is no redox process attributable to a $M^{II/III}$ oxidation couple for any of the complexes. Though the theoretical treatments suggest that the first oxidation process would indeed be metal centered, and analogous complexes such as $[RuCl(dppm)_2{=}C{=}C{=}CRPh]PF_6$ (R = Me, Ph) show an anodic oxidation process ascribed to the $Ru^{II/III}$ couple,[51] it has not been possible to observe such an oxidation process for these complexes within the spectral windows utilized.

Theoretical Considerations. DFT calculations were pursued on structure $[\mathbf{2}]^q$, for $q = -1, 0, +1, +2$. Calculations on all charge states, without symmetry constraints and with moderately asymmetric starting geometries, collapsed to structures having apparent C_{2v} symmetry and accordingly this symmetry constraint was applied in subsequent calculations. The initial C_{2v}-symmetry vacuum-phase calculations indicated that the lowest energy electronic configuration of the monocation is $[54a_1^2\ 35a_2^2\ 49b_1^2\ 39b_2^2]$, excluding those molecular orbitals arising from the "frozen core" assigned to the various atoms. Several other electronic configurations of this charge state (with both singlet and triplet multiplicity) were also investigated, but all were found to lie at least 0.5 eV above this specified ground state configuration at the PBE/(TZP, DZ) level of theory. An energy level diagram for the ground state monocation is shown in Figure 7. The energies of the excited state configurations of the monocations, relative to the ground state (provided in the Supporting Information), are broadly consistent with the orbital energies shown in Figure 7. Several configurations of the neighboring charge states were also investigated and are also summarized in the Supporting Information.

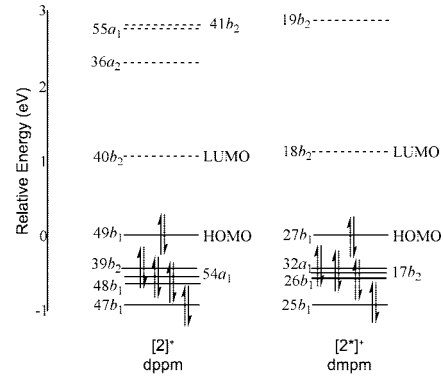

Figure 7. Computed ground-state electronic configurations of $[\mathbf{2}]^+$ and the methylated derivative *trans*-$[RuCl(dmpm)_2{=}C{=}C{=}(4,5\text{-diazafluoren-9-yl})]^+$, $[\mathbf{2^*}]^+$.

Again, the results for relative energies within each charge state are generally consistent with the orbital energies calculated for the ground state of the monocation. For all configurations surveyed, the Cα−Cβ bond length is shorter than the Cβ−Cγ bond length, by an increment ranging from 0.05 to 0.18 Å. The difference between Cα−Cβ and Cβ−Cγ bond lengths is comparatively minor in the lowest energy mono- and dicationic configurations, but a marked and progressive shift from cumulenic to acetylenic character is evident on electron addition to the monocation, with the most extreme Cα−Cβ contraction and Cβ−Cγ elongation seen in the lowest energy configuration of the anion. This geometric picture is supported by perusal of the Mulliken unpaired spin densities on various atoms, for the open-shell configurations: addition of an electron to the LUMO ($40b_2$) of the monocation is accompanied by high unpaired spin densities on Cα and Cγ, of $\mu_D = 0.27$ and 0.31, respectively (and only modest spin densities on other atoms), suggesting that reduction of the monocation is ligand-centered. Analysis of the electron density changes between different configurations (using both the Mulliken and Voronoi descriptions of effective atomic charge) essentially supports this interpretation. In contrast, removal of an electron from the HOMO ($49b_1$) of the monocation results in a preponderance of unpaired spin density on Ru and on Cβ ($\mu_D = 0.41$ and 0.32, respectively).

Comparison of relative energies *between* charge states shows the expected trend (for vacuum-phase species) in the sense that the ionization energy (IE) of the monocation exceeds its recombination energy (where the recombination energy corresponds to the neutral's IE), while the IE of the neutral also exceeds its calculated electron affinity. However, these values are not expected to correlate to the solution-phase electrochemistry of the monocation, and to this end it was judged necessary to perform solvent-corrected calculations, using the COSMO technique. Solvent-corrected calculations on the full structure, using COSMO, were not feasible with the available computa-

tional platforms, due to memory and CPU time constraints. This problem was addressed, in a reasonably satisfactory manner, by using instead a "methylated" structure [ClRu($Me_2PCH_2PMe_2$)$_2$=C=C=(4,5-diazafluoren-9-yl)]^q ($q = -1, 0, +1, +2$), [**2***]^q, in which the eight bulky phenyl groups within the diphenylphosphino moieties were replaced by methyl groups. Vacuum-phase calculations on this methylated structure suggest that it forms a quite satisfactory model for **2**. Relative energies of the frontier orbitals (and, in most cases, also those orbitals near the frontier) agree very well between the two structures, as attested by Figure 7, and the energetic and key geometric properties of the two structures, in various charge states and electronic configurations, also exhibit quite close correspondence. The ground state monocationic electronic configuration of **2*** is [$32a_1^2$ $13a_2^2$ $27b_1^2$ $17b_2^2$]. The principal difference between the two species, from an electrochemical perspective, appears to be that **2*** does not feature any isolable neutral or anionic stationary points corresponding to electron addition to the LUMO+1 ($36a_2$) of **2**. However, this "point of orbital variance" is not expected to greatly distort the electrochemistry of the smaller model versus that of the larger structure, since the $36a_2$ orbital is more than 1 eV above the $40b_2$ LUMO of **2** and does not feature in either the neutral or anionic ground state electronic configuration. A small but consistent structural difference between the methylated and phenylated complexes is that **2*** possesses, in all configurations surveyed, a longer Ru−Cl bond than **2**. For other central bond lengths, the variation between the configurations is smaller and does not appear systematic.

Having established that a methylated species could serve as a satisfactory model to the full structure, single-point COSMO calculations were then performed on the vacuum-phase optimized geometry for each electronic configuration of each charge state, for dielectric constant values of $\epsilon = 4$ and 10. The results of these calculations are provided in the Supporting Information. The application of solvent corrections does not overturn the identity of the lowest energy electronic configuration for any charge state, at either ϵ value sampled. However, a satisfactory interpretation of the computed data is hindered by the observation that the calculations reveal electron addition to the monocation to be endothermic at $\epsilon = 10$ (electron addition to a monocation should always be exothermic, regardless of the surrounding medium's dielectric constant), while the neutral is also found to be averse to electron addition. A plausible reason for this problem is that the evaluation of relative energies here uses geometries optimized in the vacuum phase: if the solution-phase geometries are markedly different, then the relative energies of different charge states are quite likely skewed by the use of these vacuum-phase geometries in single-point solvent-corrected calculations.

Solvent-corrected geometry optimizations were pursued on **2***, again using both $\epsilon = 4$ and 10, although it was found that for $\epsilon = 10$ (and for anions at $\epsilon = 4$) all configurations exhibited loss of chloride. To address this problem, the relative energies for $\epsilon = 10$ have been obtained through single-point calculations at this dielectric constant, using geometries optimized at $\epsilon = 4$. Relative energies of the various mono- and dicationic configurations were generally not greatly affected by the change from vacuum-phase to solvent-corrected ($\epsilon = 4$) optimized geometries. Absolute energies at $\epsilon = 4$ are systematically lower when $\epsilon = 4$ optimized geometries are employed than when the geometries are vacuum-phase-optimized, as is to be expected: in general, the rearrangement from vacuum-phase-optimized to solvent-optimized geometries releases up to ~30 mhartrees (ca. 75 kJ mol^{-1}) of energy at this value of the dielectric constant. The $\epsilon = 10$ absolute energies are also found to be systematically lower when geometries are optimized at $\epsilon = 4$ compared against the vacuum-phase geometries, indicating that the $\epsilon = 4$ geometries provide a closer approximation to the "true" $\epsilon = 10$ geometries.

How can the geometric trends for the $\epsilon = 4$ optimizations be interpreted? The loss of chloride from the complex on reduction is inconsistent with the experimental finding that the second reduction of **2** is reversible. However, it may well be that the chloride is intrinsically less strongly bound to ruthenium in the methylated species **2*** than in the phenyl derivative **2** (which would be consistent with the differences in optimized vacuum-phase geometries for these species, as noted above). It is also quite possible that the much greater steric bulk of arrayed phenyl groups in **2** effectively prevents solvation of the chloride ion in a manner not possible in the relatively unhindered structure of the methylated species. Thus the computational result that [**2***]$^-$ is unstable against chloride loss can quite likely be reconciled with the experimental indication that the structural integrity of [**2**]$^-$ is maintained. In any event, comparison of vacuum-phase and solvent-corrected geometries shows that the Ru=Cα and allenic C=C bond lengths are not greatly affected by solvation; nor are these bond lengths much different between the phenyl and methyl derivatives. Consequently, we expect that the trend seen on reduction in the vacuum-phase calculations (namely, contraction of Cα=Cβ and elongation of Cβ=Cγ) should hold also in the solvated system.

Summary and Conclusion

We have demonstrated that with careful choice of substituent one can construct a suitably substituted alkynol that yields diazafluorenyl allenylidene complexes of group eight. We have not been able to produce a bis-allenylidene complex by applying the standard Selegue protocol in these ionic systems and we will continue to extend our search to other systems to fulfill this goal.

The effect of the variation in metal and ligand on electronic and electrochemical characteristics of these complexes has been investigated by using UV–vis, solution electrochemistry, and a combination of these techniques in spectroelectrochemical experiments. DFT calculations on *trans*-[RuCl(P∩P)$_2$=C=C=(4,5-diazafluoren-9-yl)]^q (P∩*P* = dppm, dmpm; $q = -1, 0, +1, +2$) and subsequently solvent-corrected calculations with use of COSMO were also undertaken to examine the nature of electronic transitions in various oxidation states. However, satisfactory interpretation of the computed data (and thus analysis of the spectroelectrochemical data) was hindered by the calculated endothermicity of electron addition to the monocation when solvent corrections were included. Neglect of solvent effects led to a result that, instead, appeared qualitatively correct.

Acknowledgment. The authors wish to acknowledge the ARC for funding and provision of fellowships to M.G.H. and M.P.C. and APA scholarships to N.A.L, V.S., and P.A.S. Use of the ChemMatCARS Sector 15 at the Advanced Photon Source was supported by the Australian Synchrotron Research Program, which is funded by the Commonwealth of Australia under the Major National Research Facilities Program. ChemMatCARS Sector 15 is also supported by the National Science Foundation/Department of Energy under grant nos. CHE9522232 and CHE0087817 and by the Illinois Board of Higher Education. The Advanced Photon Source is supported by the U.S. Department of Energy, Basic Energy Sciences, Office of Science, under Contract No. W-31-109-Eng-38.

Supporting Information Available: Results of DFT calculations (vacuum phase PBE calculations on [**2**]^q and [**2***]^q, single-point solvent-corrected PBE calculations on [**2***]^q, and Cartesian coordinates for the vacuum-phase optimized geometries of [**2**]^q), UV–vis spectroelectrochemical plots for **2**, and additional crystallographic data for **3** and **4**. This material is available free of charge via the Internet at http://pubs.acs.org. CCDC 652281–652285 contains the supplementary crystallographic data for this paper. These data can be obtained free of charge from The Cambridge Crystallographic Data Centre via www.ccdc.cam.ac.uk/data_request/cif.

OM700824G